Arch Jap Chir 47 (3), 259~279, Mai, 1978

原　　著

Ultrastructural basis of Blood-Synovial Barrier

——Results with five electron-opaque tracers——

CHIAKI HAMANISHI

Department of Orthopaedic Surgery, Faculty of Medicine, Kyoto University
(Director : Prof. Dr. TAKAO YAMAMURO)
Received for Publication Feb. 3, 1978

The selective permeating mechanisms for plasma proteins termed the Blood-Synovial Barrier (BSB) were studied ultrastructurally using five different molecular sized electron-opaque tracers ; horseradish peroxidase, beef liver catalase, ferritin, dextran 200, and shellfish glycogen. The tracers were injected via the tail vein of mice and observation were made from fifteen seconds to ninety minutes after injection. Three stages of the BSB such as vascular endothelium (first), perivascular basement membrane (second), and cellular incorporation by macrophages and lining "A" cells (third) were clearly outlined in this study. The "excluded voume effect" of the hyaluronate-protein complexes in the synovial matrices was not evident. The diaphragmed fenestrations did not allow free permeation of any tracer.

Introduction

Protein molecules contained in normal synovial fluid are mainly derived from plasma proteins, however, there are definite differences in concentration and electrophoretic distribution of proteins between the plasma and synovial fluid. Total protein of synovial fluid is about one-third that of total plasma protein. The percentage of albumin is higher (65-80%) while that of γ-globulin is lower (6-12%) in normal synovial fluid than in normal plasma[19]. The decrease in larger molecular size proteins in synovial fluid is directly proportional to the size and weight of protein molecules[12] and the average concentration of α-2 macroglobulin and IgM is in the range of only 3 to 5% of those in plasma. Fibrinogen is not detectable in normal synovial fluid[22]. The mechanisms by which the normal synovial tissue excludes plasma proteins of larger molecular size or of asymmetic shape are not well understood. However, numerous speculations have attributed these mechanisms to the endothelium of small vessels, to the presence of macromolecules of hyaluronate-protein complexes in the matrices and synovial fluid, or to both. Many experiments using different

Key words : Blood-Synovial Barrier, Electron-opaque tracers, Excluded volume effect, Fenestrated endothelium.

Present address . Department of Orthopaedic Surgery, Kyoto University Hospital, Sakyo-ku, Kyoto 606, Japan.

electron-opaque tracers, such as iron dextran[3], carbon[1], and colloidal gold[28] have been done to investigate the functions of the synovial lining cells and the permeability of matrices. These tracers were injected intra-atricularly. SHANNON and GRAHAM[23] observed the massive incorporation by the synovial "A" cells of three types of peroxidase given intra-articularly, and suggested that this incorporation may be to some extent participate in barrier mechanisms. Mercury sulfide, throtrast and ferritin[6] have also been used as tracers and were administered intravenously. SHUMACHER[21] mentioned the leakiness of venules and active phagocytic activities of the endothelium of small synovial vessels as determined by intravenously injected ferritin and carbon. The hyaluronate solution acts like a sieve or a three dimensional network of stiff chains, to form an obstacle to the diffusion of larger particles (sieving effect), and to exclude other molecules from the area it occupies[15] (excluded volume effect). NETTELBLADT and SUNDBLAD[14] repeatedly filtered normal serum using hyaluronate firm gel and obtained filtrates with a protein concentration similar to that seen in the normal synovial fluid (packed volume effect). These effects may account in part for the low concentration of larger molecular weight or asymmetric shape proteins in the synovial fluid. In many of the synovial superficial capillaries, grouping fenestrations have been observed [15][29], but the functions of this structure have not been entirely elucidated. SIMKIN and PIZZORNO suggested that such may be an adaptation designed to restrict the passage of proteins and promote the rapid interchange of fluids and small molecules[27]. Using electron-opaque tracers of five different sizes, shapes, weights, and which were differently electrically charged, we investigated the morphological basis of the Blood-Synovial Barrier. In some experiments, ruthenium red was used to stain the acid mucopolysaccharides in the synovial matrices.

Materials and Methods

1. Animals; Male and female ICR and d-d strain mice 3-4 months old and weighing 30-40g were used.

2. General; 0.2 to 0.5ml of each tracer solution dissolved in isotonic saline was injected via the tail vein into unanesthesized mice. The animals were sacrificed by neck dislocation at 15 seconds to 90 minutes after the injection. The skin of both knee joints of mice sacrificed within 2 minutes after injection were incised and the fixative was injected into both knee joints immediately. Both knee joints of all mice were dissected *en bloc* with bones and capsule, and immersed in the fixative for two hours at 4°C. The capsule together with the synovium was excised as one block as shown in Fig.1, and chopped manually into small blocks of 0.5 0.5×1mm in such a way that the synovial lining cell layers were contained in each block. Fifty to sixty blocks could be obtained from both knee joints. Small blocks were then fixed for another two hours. If bleeding occurred in the synovium during intra-articular injection of the fixative, these joints were excluded from the experiments. For the fixation described above, 2.5% glutaraldehyde solution in 0.1M cacodylate buffer, pH 7.3, or 2% paraformaldehyde - 2.5% glutaraldehyde mixture in 0.1M cacodylate buffer, pH7.3, containing 0.4% $CaCl_2$ was used. In the experiments using dextran 200 or glycogen,

the one step fixative method was used[24]. The final composition of this fixative was 1.5% paraformaldehyde, 2.5% glutaraldehyde, 0.67 % osmic acid and lead citrate (2-3mg/100 ml) in 0.1M phosphate buffer, pH 7.4. Tissue blocks were washed overnight in 0.1M cacodylate buffer at 4°C. Peroxidase or catalase injected blocks were incubated in each histochemical medium as described in paragraph 3. They were then postfixed with 1% osmic acid in 0.1M phosphate buffer, washed, rapidly dehydrated in graded ethanols, and embedded in Epon 812 or Quetol 651. All specimens were embedded in flat molds so that a suitable orientation of the lining cell layers and basal tissues for transverse sectioning could be obtained. Thick sections (0.5–1 micron) were stained with toluidine blue, observed under a light microscope, and capillary rich portions of lining cell layers were selected. Sections showing silver to gold interference colors were cut with glass knives on a MT-2 Porter-Blum ultramicrotome and observed under a Hitachi 11D-S electronmicroscope.

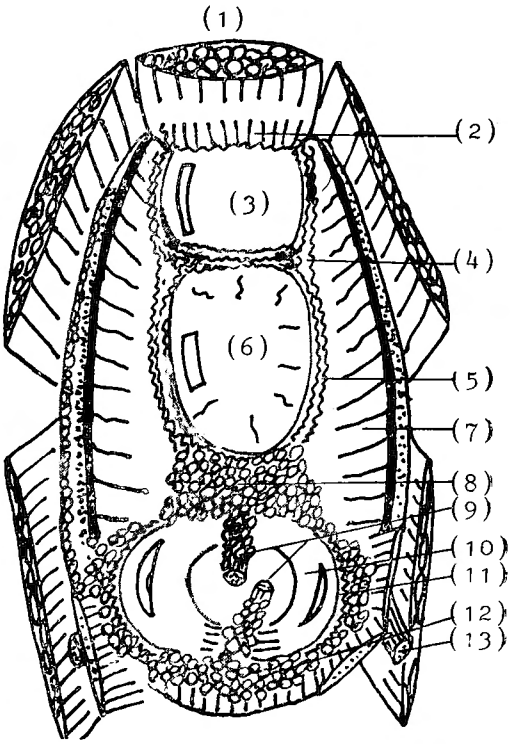

Eig 1. Excised knee joint capsule (from posterior)
(1) M. quadriceps (Vastus intermedius)
(2) Supra-patellar muscular type synovium.
(3) Cartilaginous patella.
(4) Inter-patellar villous type synovium.
(5) Peri-patellar synovial folds. (Villous type synovium)
(6) Bony patella.
(7) Condylar fibrous type synovium.
(8) Inter-condylar fatty pad. (Fatty type synovium)
(9) Cruciate ligaments.
(10) Meniscus
(11) Root of meniscus. (Fatty and villous type synovium)
(12) Fatty pad in posterior articular cavity.
(13) Collateral ligament.

3. Experiments with tracers

1) Horseradish peroxidase: Five to seven milligrams of Sigma type II peroxidase (RZ value 1.0–1.5, Sigma Chemical Co., St. Louis, Mo.) dissolved in 0.5ml of isotonic saline were injected. At time intervals of 15, 30 seconds, 1, 2, 3, 5, 8, 10, 15, 30, 60, 90 min. after injection, fixation was initiated. Three different methods for fixation were carried out.

1. Intra-articular injection of fixative immediately after sacrificing mice, killed within 2 min. after injection.

2. Intravenous injection of 0.3 ml of fixative via the same vein 15 and 30 sec. after injection of peroxidase. This volume of fixative was lethal and the extremities became rigid immediately as a result of fixation of vascular beds.

3. *En bloc* immersion fixation of the dissected total knee joint blocks with bones and capsule for 2 hours followed by excision of synovium from partly fixed joint blocks. This

method for fixation was performed for most of the mice sacrificed later than three minutes after injection, because there was no risk of extravasation of intravascular tracers by direct intra-articular damage. Excised and chopped synovial blocks were re-fixed, washed overnight, immersed in Tris-HCl buffer, pH 7.6, for 30min., and incubated in GRAHAM-KARNOVSKY's medium[7] for 10 to 15 min. at a room temperature of 15°C, to demonstrate peroxidatic activity. This medium contained 5mg of 3,3' diaminobenzidine-4HCl and 0.1ml of 1% H_2O_2 in 9.8ml of 0.1M This-HCl buffer, pH 7.6. Washed blocks were then postfixed for 1 hour with cacodylate buffered 1% osmic acid. The ultrathin sections were examined without counterstaining by heavy metals.

2) Catalase : Twenty milligrams of twice-crystallized beef liver catalase (Sigma Chem. Co., Stock No. C-105) in 0.5ml of aqueous solution were injected very slowly into the tail vein of each unanesthetized mouse. To obtain a higher concentration of catalase, approximately one-half of the supernatant was removed from the stock solution before dissolving the enzyme by sonication at 37°C. At time intervals of 1, 3, 5, 10, 15, 40, and 60 min. after injection, the synovium was fixed and processed as in the experiments with peroxidase. Chopped tissue blocks were incubated in the medium described by VENKATACHALAM and FAHIMI[31] for 2-4 hours at a room temperature of 15°C. This medium consisted of 10mg of 3,3' diaminobenzidine-4HCl, 10ml of 0.1M Tris-HCl buffer, pH 8.5, and as a peroxide source, 25mg of barium peroxide in a dialysis bag.

3) Ferritin: Twenty-five to fifty milligrams of cadmium-free ferritin in 0.25-0.5ml of aqueous solution (twice-crystallized, ICN pharmaceuticals Inc., Cleveland, Ohio. Lot No. 1693) were injected very slowly into the tail vein of each unanesthetized mouse. At time intervals of 2, 5, 10, 15, 30, and 60 minutes after injection, the knee joints were fixed *en bloc*. The procedures were the same as specified in paragraph 2. Potassium ferrocyanide was added to the osmic acid for the postfixation. The ultrathin sections were examined after staining with bismuth nitrate[2]. In some tissues, staining of hyaluronateprotein complexes with ruthenium red was also done concomitantly.

4) Dextran 200: 0.3ml of 10% (w/v) dextran 200 solution (Nakarai Chem. Ltd., Kyoto) dissolved in isotonic saline was injected. At time intervals of 3, 5, 10, 20, 30, and 60 min. after injection, the mice were sacrificed and one step fixative was injected into both knee

Table. 1. Molecular properties of tracers and plasma proteins

	M. W.	Diameter	Shape	Charge	E.D.R.***
Peroxidase	40,000	50Å	Symmetric	7.2	25−30Å
Catalase	240,000	240Å*	Ellipsoid (1:5)**	5.6	52Å
Ferritin	480,000	110Å	Symmetric	4.1−4.6	61Å
Dextran 200	200,000	90−230Å	Globular		100Å
Glycogen	−1,000,000	180−400Å	Globular		
Albumin	69,000	150Å*	Ellipsoid (1:4)**	4.6	
γ-globulin	160,000	230Å*	Ellipsoid (1:5)**	6.4−7.2 (IgG: 7.3−8.2)	
Fibrinogen	400,000	680Å*	Ellipsoid (1:20)**	5.5	

* long diameter, ** short diameter : long diameter *** effective diffusion radius

joint cavities. Excised and chopped synovium were immersed in the fixative for an additional 2 hours, dehydrated, and embedded in Quetol 651.

5) Glycogen: 0.3ml of 15% (w/v) shellfish glycogen (Nakarai Chem. Ltd.) dissolved in isotonic saline was injected. At time intervals of 5, 15, 30, and 60 minutes after injection, intra-articular fixation with one step fixative was begun. The following steps were the same as in the experiments with dextran 200. Molecular properties of tracers and some plasma proteins were shown in Table 1.

4. Experiments with ruthenium red

Twenty-five milligrams of ferritin were injected intravenously. Five and twenty minutes after injection, the mice were sacrificed and the synovium were excised and chopped. Tissue blocks were processed as described by HIGHTON and MYERS[10], in which these blocks were fixed with 2.5% glutaraldehyde containing 1500 ppm of ruthenium red (Chroma-Gesellschaft, Stuttgart), washed with buffers containing 800ppm, postfixed with 1% osmic acid containing 400 ppm of ruthenium red, dehydrated and embedded in Quetol 651.

5. Control experiments

1) Endogenous peroxidatic and catalytic activities: The synovium of mice injected with 0.5ml of isotonic saline were incubated in each medium which is specific to demonstrate the peroxidatic or catalytic activity. The procedures were the same as specified in paragraph 3, 1) or 2).

2) The effects of increased plasma volume: The ultrastructure of the synovial vessels of mice injected with 0.5ml of isotonic saline were compared with that of untreated mice

3) Experiments for assessment of vascular leakage induced by histamine: Mice were injected intravenously with Evans blue, and were then given subcutaneously 20 micrograms of each tracer. The blue area produced was measured and compared to that produced with isotonic saline and 20 micrograms of histamine.

Results

Ultrastructures of the synovial membrane

1. Type of synovium

Four types of synovium such as fatty, fibrous, muscular, and villous type were observed. (Fig.2)

1) Synovium of fatty type: This type was found as the fatty pads and was most voluminous in the knee joint. In Fig. 1, this type of synovium was located in the area (8),(11), and (12). The lining cell layer was composed of one to three layers of lining cells and fenestrated type capillaries and was supported by the fatty tissue. (Fig. 2A) The endothelium of the capillaries running through the inter-fatty lobular matrices was mainly of the continuous type. The extent of the vascular bed in this type of synovium was far larger than that of other types. Thus the manifestation of edema or swelling were earliest when there was an increase in vascular permeability such as antigen-induced arthritis of mice using methylated-BSA as antigen (in preparation).

2) Synovium of fibrous type: In Fig. 1, the condylar area (7) largely belong to this type. One to two layers of lining cells covered the joint capsule or the ligaments. (Fig. 2B) The lining cell layers had collagen-rich matrix and fewer capillaries of the fenestrated type.

3) Synovium of muscular type: This type was found at the innermost layers of the vastus intermedius muscle (Fig. 1-(2)). One to two capillary-rich lining cell layers covered the muscle. (Fig. 2C) Nerve fibers were often observed.

4) Synovium of villous type: This type was frequently seen as a few synovial folds at the transitional area between synovium and perichondrium (Fig. 1-(5) and (11)). The villi were composed of two to six layers of lining cells (Fig. 2D), numerous small vessels, and lymphatic channels. In antigen induced arthritis, the inflammatory cellular infiltration was the most prominent and earliest in this type of synovium (in preparation).

2. Synovial lining cells

The three types of cells observed in the synovial lining cell layers were termed "A", "B", and activated "B" or "C" respectively.

1) Type "A" cells: The most characteristic features were the numerous thin and long cytoplasmic processes (filopodia) which engulfed massive tracers and fused to form large phagosomes. (Fig. 5E, 5G, 7D, 7E) The "A" cells located adjacent to the capillaries extended their filopodia to the capillaries. The uppermost layer of synovium was, in many parts, covered by thin long extended filo-

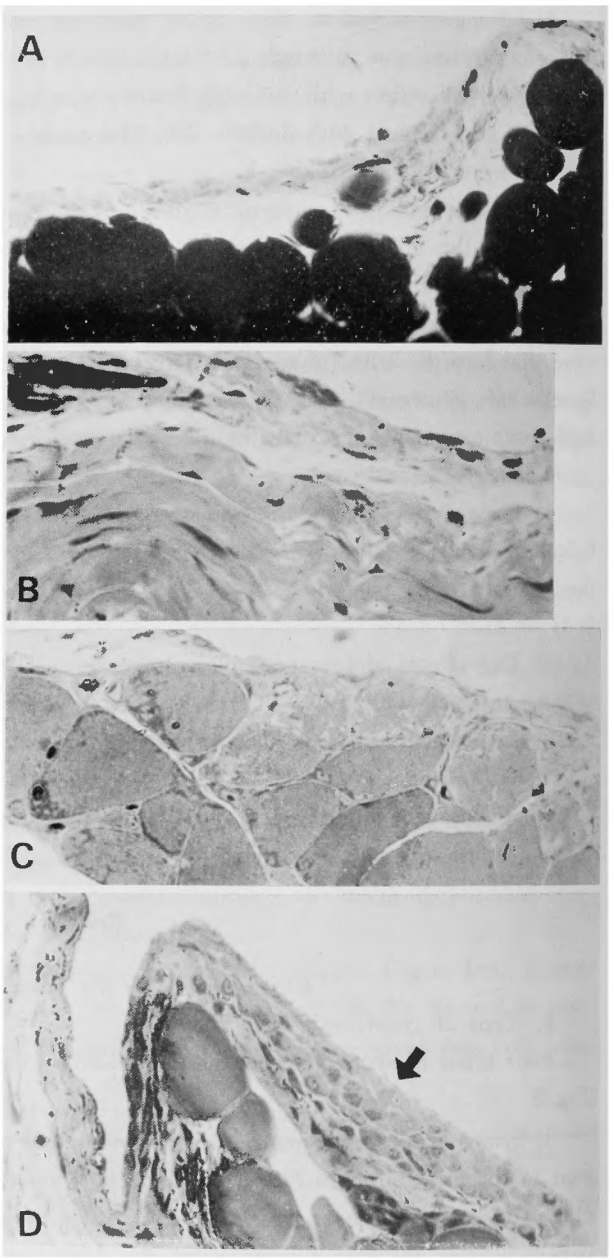

Fig 2. Four types of synovium.

(Fig A) Fatty type synovium. ×240
(Fig B) Fibrous type synovium. ×240
(Fig C) Muscular type synovium. ×240
(Fig D) Villous type synovium. 4~6 layers of lining cells. Arrow indicates the guitar shaped "C" cell, ×280

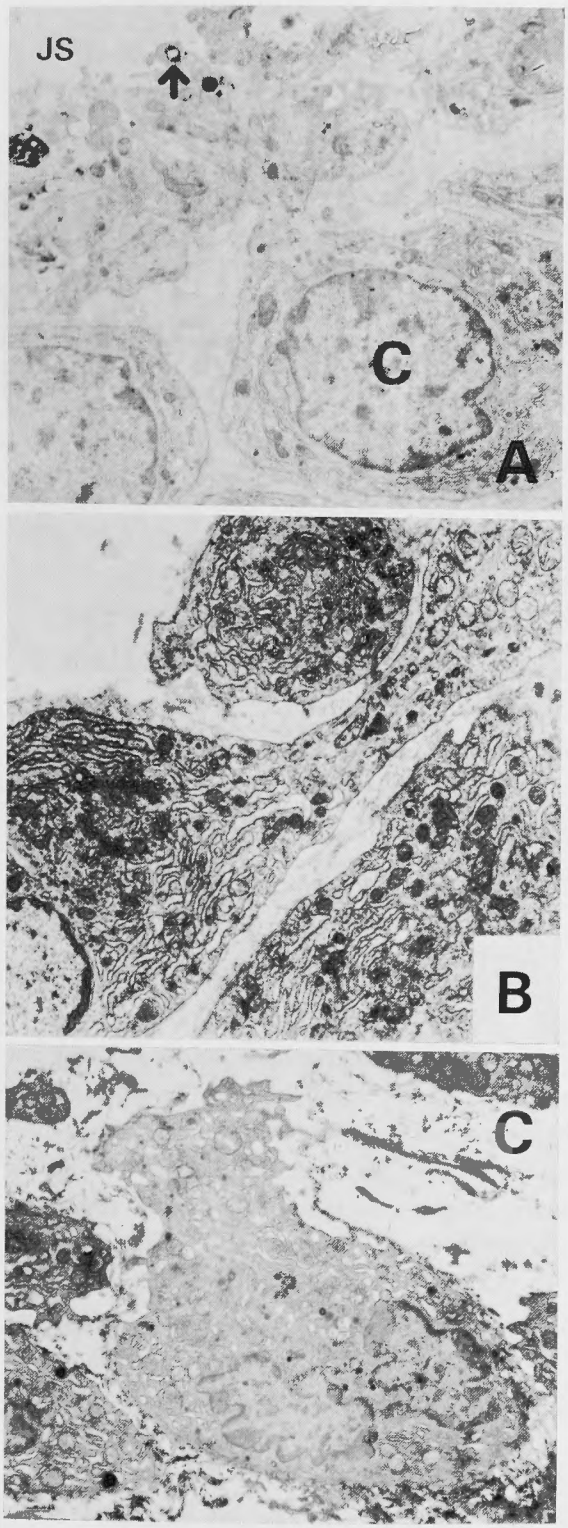

Fig 3. Type "C" or activated "B" type lining cells observed in antigen-induced arthritic condition using m-BSA as antigen. Acute inflammatory phase.

(**Fig A**) Typical wine-cup shaped "C" cell. The head portion facing the joint space (JS), is rich in mitochondria and filopodia. Arrow indicates the vesicular incorporation of intravenously injected peroxidase. ×5,250

(**Fig B**) Bottle shaped "C" cell. The neck portion contains numerous microfibrils. Markedly developed Golgi apparatus and rough ER are observed in the basal portion. ×6,340

(**Fig C**) This "C" like cell is binucleated. Adjacent matrix is markedly edematous. ×4,000

podia of "A" cells.

2) Type "B" cells: The cell membrane was smoother with fewer cytoplasmic processes. (Fig. 5G) Numerous pinocytotic vesicles were observed in the peripheral cytoplasm. The most conspicuous were the large number of elongated cisternae of rough endoplasmic reticulum. Abundant microfibrils were usually seen in the cytoplasm.

3) Type "C" cells: This type of cell was conspicuously and characteristically bottle, guitar, or wine-cup shaped (Fig. 3). The head portion of this cell faced towards the joint space and was rich in mitochondria, microfibrils, cytoplasmic processes and vesicles which often incorporated peroxidase (Fig. 3A). The nucleus and the large number of rough endoplasmic reticulum were located in the basal portion. In spite of "A" cell like functions, this type of cell was considered not to be a transitional type between "A" and "B", but a subtype of "B" cell with more active functions. These "C" cells could be found more frequently under inflammatory conditions (in

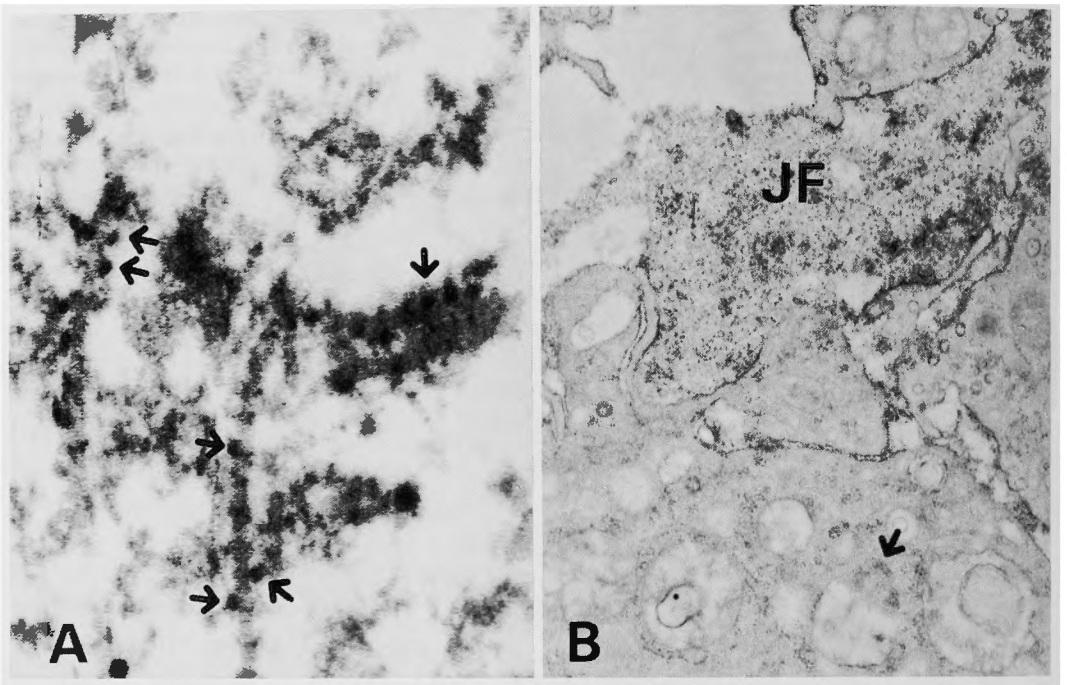

Fig 4. Ruthenium red stainng of the synovial matrix.

(**Fig A**) Ruthenium osmium positive globules are aligned on each collagen fiber with same periodicities (arrows). The mean diameter of these globules is 320Å. These appeared to be the bridging proteins of proteoglycan. ×62,000

(**Fig B**) Twenty minutes after injection of ferritin. Arrow indicates incorporated ferritin particles in the phagosomes of "A" cell. Ruthenium osmium positive particles are dispersed in the joint fluid (JF) diffusely and are observed also in pinocytotic vesicles. ×18,600

preparation),

3. Inter-lining cellular matrices

Lining cells were only loosely arranged in the intercellular ground substances and did not form any kind of direct inter-cellular connection like tight junctions or desmosomes. No true basement membrane separated the lining cell layers from the underlying supporting tissues. The distance between lining cells varied from 0.1 to 1 micron. The matrix stained with ruthenium red showed a more intense staining of the dense ruthenium osmium positive materials aligned on the collagen fibers with same periodicities (Fig. 4A) and dispersed in the joint fluid (Fig. 4B). These ruthenium positive materials were composed of glubular particles 150 to 300Å in diameter, and filamentous structures radiating from the particles. These particles and filamentous structures were assumed to be proteoglycan (hyaluronate-protein complexes) such as are seen in the matrices of cartilage[9].

4. Small vessels

The lining cell layers and underlying fibrous, fatty, and muscular tissues had each vascular plexus. The endothelium of capillaries penetrating the lining cell layers was often

attenuated markedly and formed many fenestrations (Fig. 5C, 7B, 7E, 8). These apertures were 500 to 600Å in diameter and were mostly closed by thin diaphragm of about 40Å in thickness. As a whole, fenestrations were located on the side facing the joint space, and the nucleus and organellas were contained in the most remote portion. Continuous and vesicle-rich endothelium was often observed in the deep lining cell layers (Fig. 5B, 7C). The inter-endothelial junctions of synovial small vessels were about 0.2 to 1 micron in length and had a slit of 100 to 150Å in width (Fig. 5A, 5B, 6C, 7A). The narrower portions were observed in every junction, but in synovial membrane, those narrower portions were not occluded completely and the slit appearance was maintained at least 30 to 40Å in width. The diameter of the pinocytotic vesicles varied from 500 to 1000Å. No difference was observed between the ultrastructure of small vessels in the synovium of mice injected with isotonic saline and that of non-treated mice. Endothelial change such as sweling, loosening or gap formation of the inter-endothelial junction was never apparent.

Experiments with tracers

1. Horseradish peroxidase

Horseradish peroxidase acted on the substrate H_2O_2, and oxidized diaminobenzidine (DAB) in the incubation medium. The presence of enzyme at a particular site could be detected by these polymerized DAB and appeared as a brown reaction product under light microscope and as a black granular reaction product under electronmicroscope after osmification.

Some portions in the synovium showed endogenous peroxidatic activities, i. e. red blood cells, microbodies of macrophages, lysosomes of neutrophils, peroxisomes of eosinophils, and in the thin cytoplasm of fatty cells surrounding each fatty lobules as ultra-fine black granules.

Time sequence studies are summarized in Table 2.

Table 2. Time sequence studies of peroxidase

15 sec.	Efflux of PO* through short IEJ** about 0.2μ. Mean distance of PO-loaded endothelial pinocytotic vesicles from luminal space : 0.06μ Incorporation of PO by "A" cells and MP*** as "inner coating".
30 sec.	Efflux through IEJ about 0.5μ. Mean distance of loaded vesicles: 0.12μ Moderate PO in matrices and BM*. PO had reached joint space. Massive "bulk" incorporation of PO by "A" cells and MP
1 min.	Vesicular discharge of PO to the extra-vascular space. Efflux of PO through long IEJ. Meshwork appearence of lining cell layers with intensely stained matrices. Re-uptake and reverse transport of extravascular PO.
2-3 min.	70-80% of pinocytotic vesicles loaded PO (maximum)
5-10 min.	Maximum concentration of PO in matrices. Active pinocytotic incorporation also by "B" cells. Phagolysis of PO had begun in "A" cells and MP.
90 min.	No PO was found in vascular lumina nor matrix. PO could be found in a few perinuclear phagolysosomes of "A" cells and MP.

* PO : peroxidase, **IEJ : inter-endothelial junction, ***MP : pericapillarry macrophage, *BM : basement membrane

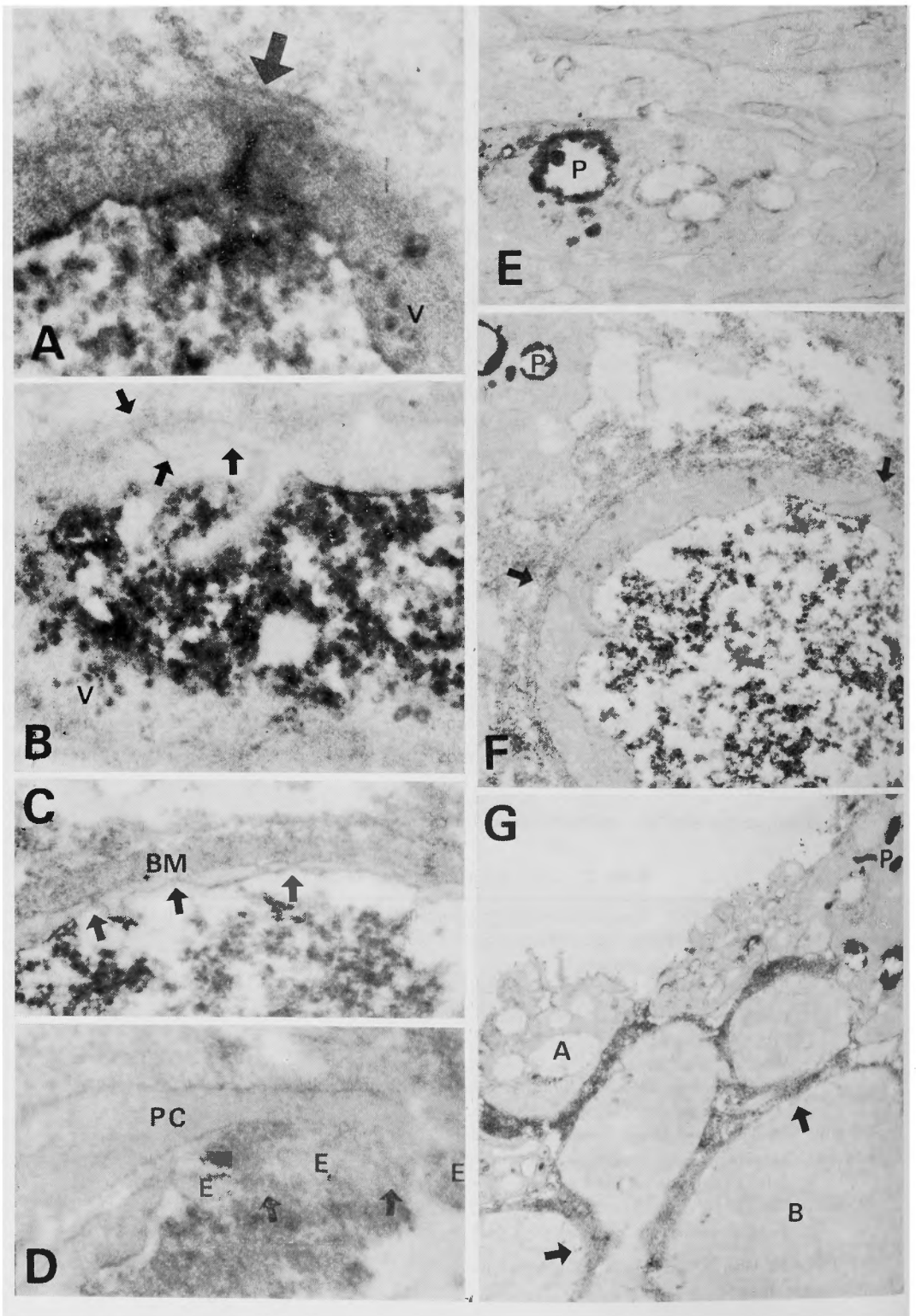
A
V
B
V
C
BM
D
PC
E
E
E
E
P
E
P
F
G
P
A
B

Fig 5. Experiments with horseradish peroxidase. No counterstaining by heavy metal.

(**Fig A**) Fifteen seconds after injection. Arrow indicates the efflux of peroxidase through the short inter-endothelial junction (IEJ) of 0.27 microns in length. Vesicular transportations (V) has begun. ×36,000

(**Fig B**) Thirty seconds after injection. Arrow indicates the efflux from the intermediate length IEJ of 0.65 microns. Many pinocytotic vesicles (V) are transporting peroxidase and almost reach the pericapillary space. ×33,800

(**Fig C**) Ten minutes after injection. Arrows indicate fenesrations. The left one may indicate the influx of peroxidase. The pericapillary besement membrane (BM) is intensely stained with the reaction product. ×38,600

(**Fig D**) Fifteen seconds after injection. Synovium with bleeding. Massive efflux of peroxidase (arrow) towards pericyte (PC) through the widened or disrupted fenestration (between E and E). ×60,000

(**Fig E**) Fifteen seconds after injection. "A" cell has already incorporated peroxidase in phagosomes (P) at this earliest time period. Phagosomes are "inner coated" with peroxidase. ×25,300

(**Fig F**) One minute after injection. Pericapillary BM and matrix are intensely stained. Arrows indicate the efflux of peroxidase through IEJ. Phagosomes of the macrophage (P) are "inner coated" ×24,500

(**Fig G**) Ten minutes after injection. The meshwork appearance of lining cell layers with intensely stained matrices. Arrows indicate the pinocytotic incorporations of peroxidase by "B" cells. Condensation and lysis of peroxidase have taken place in some phagolysosomes (P) of "A" cell. ×8,300

2. Catalase

Catalase reacted in the incubation medium making catalase-peroxide complexes which showed peroxidatic activity in alkaline condition. The endogenous catalytic activities were characteristically noted at the mitrochondrial membranes and cristae (Fig. 6A) in addition to all the portions which showed endogenous peroxidatic activities. The experiments were initiated from one minute after injection, but findings in small vessels were almost similar at any time period, even 40 minutes after injection.

* Fifteen minutes after injection Reaction product of catalase was not observed in extra-vascular spaces. Catalase could not pass through the interendothelial junctions (Fig. 6C). Only a few pinocytotic vesicles facing the vascular lumina had incorporated a small amount of catalase, but the vesicular transportation was very static and no obvious discharge towards the basement membrane was observed. Concentration of catalase in the vascular lumina was as high as that seen in the earlier time period. Catalase did not pass through the diaphragmed fenestration. Only one macrophage had incorporated the reaction product of catalase into large phagosomes (Fig. 6B) despite the complete absence of catalase in the matrices. These findings were the same thereafter, even 40 minutes after injection.

3. Ferritin

Non specifically stained ferritin particles were observed under the electron microscope as electron-opaque particles of 55Å in diameter. Spherical shell of protein, apoferritin, stained with bismuth subnitrate, showed an increased electron-opaque diameter of approximately 2-fold (100-110Å).

Time sequence studies are summarized in Table 3.

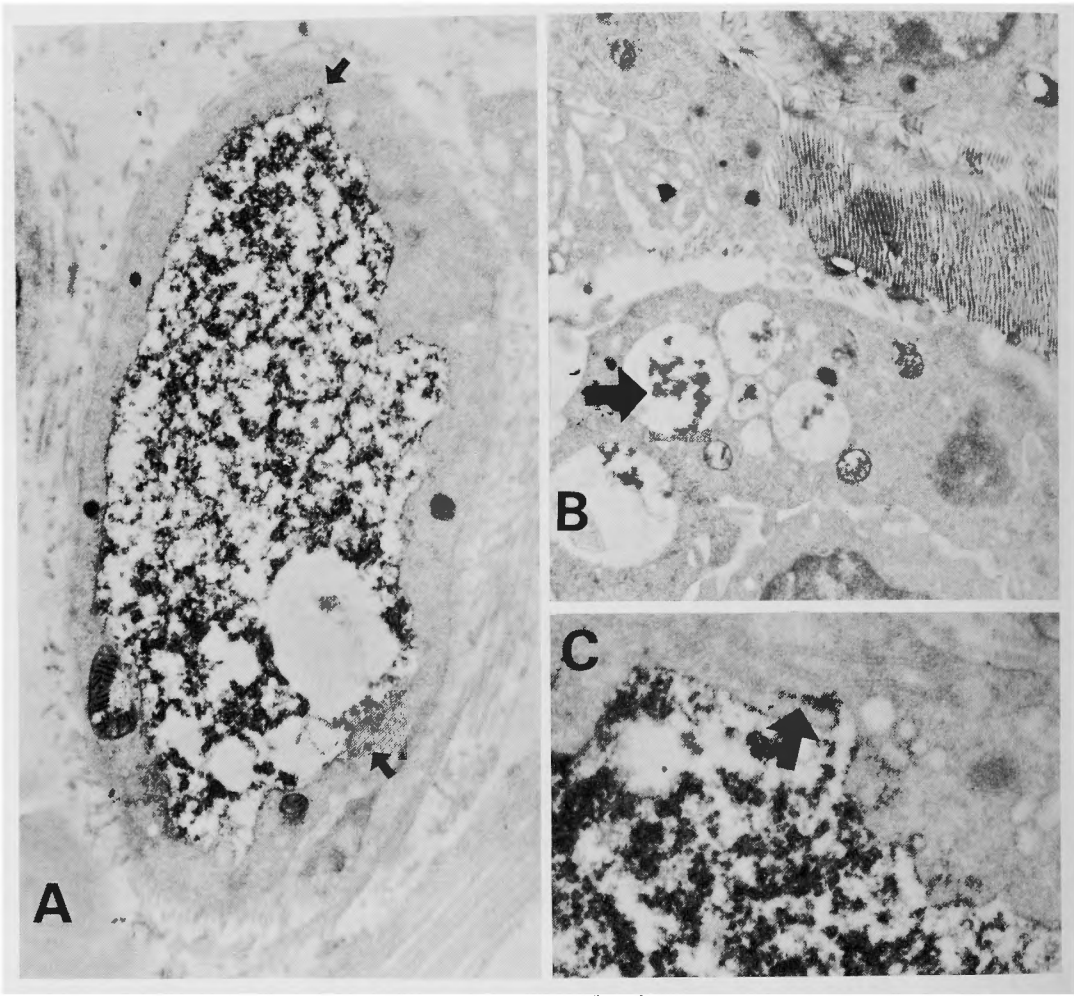

Eig 6. Experiments with catalase

(**Fig A**) Fifteen minutes after injection. Arrows indicate scarce pinocytosis of catalase. No active vesicular transportation. No catalase in extra-vascular space. Mitochondrial membrance and cristae are stained positively. ×15,000

(**Fig B**) Fifteen minutes after injection. Only this macrophage incorporated the reaction product of catalase (arrow). Extra-cellular spaces are free of catalase. ×12,600

(**Fig C**) Fifteen minutes after injection. Catalase did not pass through the inter-endothelial junction (arrow). Incorporation by pinocytotic vesicle is sparse. ×30,000

4. Dextran 200

Dextran 200 was observed under the electron microscope as nearly round particles from about 90 to 230Å in diameter. The permeation of this tracer and glycogen did not seem to be so dynamic as that of peroxidase or ferritin.

*Thirty minutes after injection: Endothelial phagocytosis of this tracer was frequently seen, but pinocytosis was rare. The tracer was discharged extravascularly and pooled vesiculously between the endothelium and basement membrane (Fig. 8A), but was not found

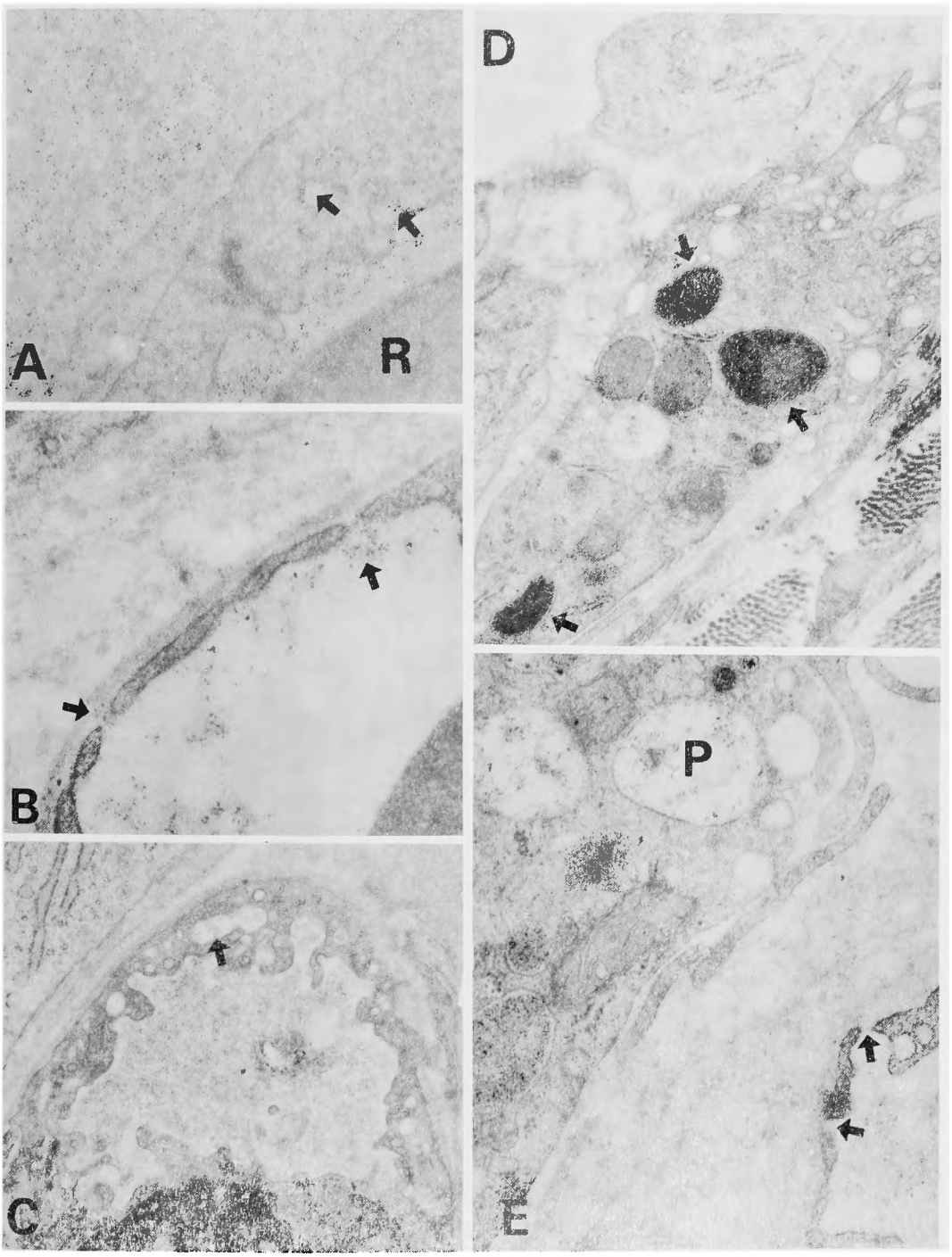

Fig 7. Experiments with ferritin

(**Fig A**) Fifteen minutes after injection. Several pinocytotic vesicles are transporting ferritin (arrows). No ferritin is found in the inter-endothelial junction. Each extravascular ferritin particle is located in close relationship with collagen fibers. R: red blood cell ×45,000

(**Fig B**) Thirty minutes after injection. Ferritin accumulates at the inside or outside of fenestrations (arrows). The number of ferritin particles in the matrix is markedly decreased as compared with Fig A. ×52,500

(**Fig C**) Thirty minutes after injection. Many ferritin particles are incorporated in some pinocytotic and phagocytic vesicles (arrow). This capillary-venule type vessel is rich in vesicles and considered to be responsible for the active vesicular transportation. ×14,000

(**Fig D**) Thirty minutes after injection. Several lysosomes in "A" cell contain numerous ferritin particles and condense them. ×19,100

(**Fig E**) Thirty minutes after injection. "A" cell adjacent to the fenestrated capillary (arrows) incorporate numerous particles in phagosomes (P) and lysosomes. ×35,300

Table 3. Time sequence studies of ferritin

2 min.	Endothelial pinocytosis, phagocytosis, and transportation. Could not pass through the IEJ*.
5 min.	Vesicular discharge to the extravascular spaces. Incorporation by macrophages and "A" cells.
15 min.	Maximum amount of ferritin in the matrix. Located in close association with collagen fibers. Dispersed in whole matrix in equal concentration.
30 min.	Condensation of ferritin in phagolysosomes. Ferritin become sparse in the matrix. Accumulation of ferritin at the inside of diaphragm of fenestration.

* IEJ · inter-endothelial junction

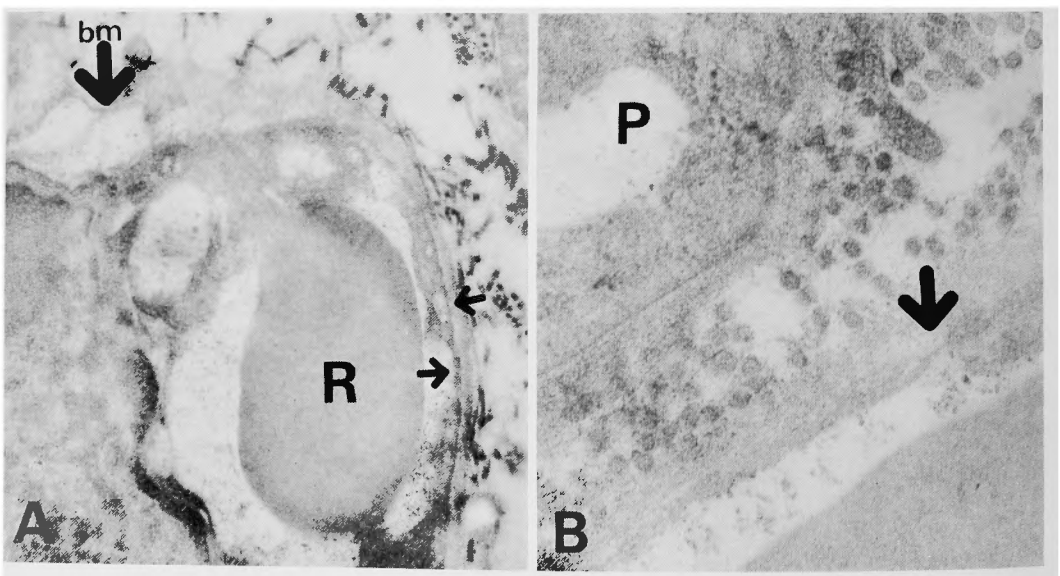

Fig 8. Experiments with dextran 200

(**Fig A**) Thirty minutes after injection. The basement membrane (bm) is ballooned and raised by dextran particles pooled below. Small arrows indicate inpermeable fenestrations (below) and phagocytic incorporation of dextran (above). No particle in the matrix. ×19,300

(**Fig B**) Thirty minutes after injection. Smaller dextran particles are observed in the phagosomes (P) of adjacent "A" cell and at the outside of fenestration (arrow). ×60,800

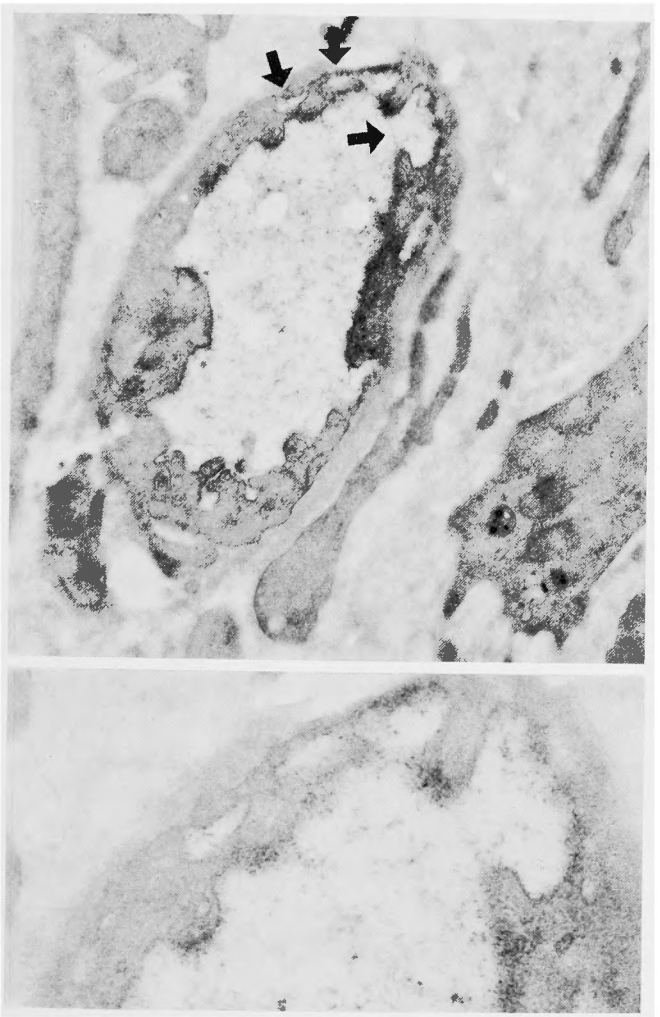

Fig 9. Thirty minutes after injection of glycogen. Marked phagocytosis are observed (arrows). No particle in the matrix. ×11,400
(below) High magnification of above. ×27,900

in the matrices. Characteristically, the basement membrane was often ballooned or raised where dextran particles were present (Fig. 8A). Macrophages and "A" cells located close to the capiliaries occasionally contained relatively small dextran particles of 100Å in mean diameter in large vacuoles. (Fig. 8B). These small dextran particles were only rarely observed also outside the fenestration.

5. Glycogen

The findings with this tracer were much the same as in the case of dextran 200. The particles were observed as globular, singly or in chain form. The diameter varied from 180 to 400Å, and the mean diameter was 230Å. Endothelial phagocytosis was frequently seen (Fig. 9) but the pooling of particles between the endothelium and the basement membrane

was less frequent than noted with dextran 200.

Discussion

1. Animals

There are several advantages in using mice as experimental animals for these studies; a) Enzyme tracers which are sensitive in small amounts can be used for large numbers of mice. These enzyme tracers has been used extensively to investigate the permeability of vessels in other organs, and it has been acertained in several strains of mice that they do not induce the release of chemical mediators which increase the vascular permeability b) Intravenous injection of tracers are easily administered through the tail vein. c) The minute size of the synovium of mice makes feasible examination of the entire synovium. One knee joint block can be dissected into only 30 small blocks.

2. Time lag

The endothelial vesicular transportation may be hastened from the time of sacrifice until fixation of the endothelium. This time lag would influence the results particularly in mice sacrificed 15 and 30 seconds after injection. SIMIONESCU and SIMIONESCU[25] studied the time lag using the skin of scrotum of rats, under vital conditions. They examined the arrest of blood flow by placing the fixative on the scrotum, and found that it took about 30 seconds. The fixative may diffuse more easily into the synovial tissue when given intra-articularly than into the cutaneous tissue, but it takes at least ten seconds to inject the fixative intra-articularly after sacrifice. To eliminate this problem, and to fix the vascular bed simultaneously with sacrifice, the fixative was given intravenously in some mice. There was a tendency for the peroxidase to be expelled forcefully into the extravascular space through the inter-endothelial junctions. This is partly due to the increase in intravascular pressure following the increased plasma volume and loss of expansibility of fixed vascular walls. However, the results concerning the vesicular transportation are probably more accurate.

3. Permeation of tracers through the endothelium

The physiologic studies by PAPPENHEIMER[16] and MAYERSON et al.[13] introduced two pathways for substances to pass through the endothelium of capillaries. One is the water-filled channel which has 30 to 45Å of effective pore radius and termed "small pore system". The other is "large pore system" or vesicular transport system, which slowly transports molecules up to 500Å in diameter. The pore theory and the vascular permeability have been studied using many electron-opaque tracers in several organs such as heart muscle[11)31)], diaphragm[25)], glomerulus[4)31)] renal tubulus[31)32)], small intestine[5)24)], lung[20)], thymus[17)], liver[8)], pancreas[32)], and iris[30)], etc. Two pore systems were also apparent in the synovium for 4 tracers except for catalase as shown in Table 4. Catalase was almost completely blocked at the level of the endothelium. The leakage of catalase through the fenestration observed in the renal tubules or the pancreas[32)] was not apparent in the synovium. When compared with ferritin, which has about a twofold molecular weight and a more negative charge than

Table 4. The pathways of tracers and Blood-Synovial Barrier

	Peroxidase	Catalase	Ferritin	Dextran 200	Glycogen
Endothelial pathways	IEJ* Pinocytotic vesicles	(Pinocytosis)	Pinocytosis Phagocytosis	Phagocytosis Frequent	Phagocytosis Occasinally
Pore theory	Small and large	(Large)	Large	Large	Large
Permeation through BM**	Freely	(No discharge towards BM)	Almost freely	Retention under BM	Inpermeable
Distribution in matrix	Diffuse No concenration gradient	No catalase observed	Diffuse No gradient	No particles	No particles
Cellular incorporation	MP** "A" and "B" Rapid and massive	One MP Exceptionally	MP and "A" Massive	Particles smaller than 200Å in MP and "A"	No obvious incorporation
Permeable fenestrations	Rare Below 2%	None	Rare Below 1%	Rare	None
Barrier sites	MP, "A"	Endothelium	MP and "A"	Endothelium BM MP and "A"	Endothelium BM
Stage of BSB	III	I	III	I, II, III	I, II

* IEJ : inter-endothelial junction, ** BM : basement membrane, ⁑ MP : macrophage

catalase, (Table 1) catalase should be able to permeate more easily than ferritin[18]. However, findings were inverse. One explanation may be that catalase is an ellipsoid shaped molecule. As shown in Table 1, the ratio of long diameter over short diameter of catalase and γ-globulin are about 5. This asymmetric shape and more negative charge than γ-globulin, probably explain why catalase cannot pass through the endothelium. Considering the permeation of ferritin and even dextran 200, it is apparent that the shape, size, and symmetry of the protien molecule are the most important factors with the molecular charge being the next, regarding permeation through the endothelium of synovial small vessels.

4. Permeation of tracers through the perivascular basement membrane and inter-cellular synovial matrix.

As shown in Table 4, free permeation of peroxidase and ferritin through the basement membrane and synovial matrix was observed. These two tracers are located in close interrelationship with collagen fibers in the matrix. The inversely proportional concentration gradient of tracers to the distance from the capillary was not evident, and such is considered to be morphologic proof of "excluded volume effect" of the hyaluronateprotein complexes in the matrix. Smaller dextran particles could pass the basement membrane and were occasionally incorporated by the macrophages. A similar relationship between molecular size of graded dextran particles and the permeability of the basement membrane was observed in the glomerulus[4] and the small intestine[24].

5. Role of fenestrated capillaries

This type of capillary ordinarily seen in the tissue which transportr water, electrolytes,

proteins or metabolic substances massively, viz, most exocrine and endocrine organs, intestinal mucosa, glomerulus, tubulus, thymus, lymph node, choroid plexus, iris, retina, gingiva and bone marrow etc. SUTER and MAJNO[29] observed this type of capillary in the synovium of rat in 1964. Many tracer studies have been done using different organs to investigate the specific permeability of this aperture and the relationship with the pore theory. It was clarified that there was much discrepancy in the frequency and permeability in each organ[26]. The frequency of fenestration in one unit area is much higher in the glomerulus and tubulus than any other organs, and the frequency of non-diaphragmed fenestration is also higher in the kidney. Free permeation of peroxidase, ferritin, several molecular weight dextrans and even catalase through non-diaphragmed type of fenestration was observed in the kidney. On the contrary, in the intestinal mucosa, the number of fenestrations is about half of that in the tubulus[26], and the frequency of permeable fenestration was variable in accordance with the molecular size of tracers[5][24].

In the present report "permeating" or "permeable" fenestration is defined as the same concentration of the tracer noted continuously from the inside to the outside of the aperture. In synovium, almost all fenestrations were closed by diaphragms, and only a few seemed to be permeable to some tracers (Table 4). But the percentage of these permeable fenestrations was below 2% of all fenestrations observed. There is much discrepancy concerning the frequency in the small intestine, reported to be from 20 to 70%[24] so that in synovium, it is impossible to define the fenestration acting as a large pore system. Massive leakage of peroxidase through some widened fenestrations was observed at some areas of bleeding due to trauma caused by needle during intra-articular injection of the fixative (Fig. 5D). On the other hand, in the acute inflammatory phase of antigen-induced arthritis, the fenestrations seemed to be intact though there are massive interstital edema and swelling of endothelium of continuous type capillary (in preparation). These findings suggest that the fenestration may be the *locus minoris resistentiae* to mechanical stimuli, is able to change to the large pore system, but may be resistant to immunological or chemical stimuli.

6. Cellular incorporation

Macrophages and "A" cells incorporated tracers at the earliest time period (peroxidase), massively (ferritin and peroxidase), and even when no obvious tracers was found in the extracellular matrices (dextran 200 and catalase). These findings suggest that the abilities of macrophages and "A" cells to migrate, engulf the extracelluar substances by extending their filopodias, and phagocytize are very dynamic and active. Whether or not the usual plasma proteins are incorporated like exogenous tracers is unknown. Nevertheless, the cellular incorporation probably participates in the Blood-Synovial Barrier.

Our findings herein clearly demonstrate that 1) the specific structures and functions of endothelium of small synovial vessels manifest either actively or passively, selective permeability to certain protein molecules, and correspond to the first stage of Blood-Synovial Barrier. 2) the findings that further permeation of dextran 200 and glycogen were blocked at the basement membrane suggest that the perivascular basement membrane acts as the

second stage of Blood-Synovial Barrier to molecules larger than about 180 to 200Å in size or 90 to 100Å in effective diffusion radius. and 3) extremely rapid and massive incorporation of tracer by the juxta-vascular macrophages and "A" cells is probably the third stage of Blood-Synovial Barrier. The "excluded volume effect" of the hyaluronate protein complexes considered to be located in the inter-lining cellular matrices was not demonstrated.

Acknowledgments

Gratitude are due to Emeritus professor T. Ito, for overall instruction, to Dr. J. Nagai, M. Ohara for pertinent discussion and assistance with the manuscript, and to K. Tsuchida for preparing the photographs.

Reference

1) Adam WS : Fine structure of synovial membrane : phagocytosis of colloidal carbon from the joint cavity. Lab Invest **15**: 680-691, 1966.
2) Ainsworth SK, Karnovsky MJ: An ultrastructural staining method for enhancing the size and electron opacity of ferritin in thin sections. J Histochem **20** : 225-229 1972.
3) Ball J, Chapman JA, et al The uptake of iron in rabbit synovial tissue following intra-articular injection of iron dextran. A light and electronmicroscope study. J Cell Biol **22** 351-364, 1964.
4) Caufield JP, Farquhar MG The permeability of glomerular capillaries to graded dextrans. Identification of the basement membrane as the primary filtration barrier. J Cell Biol **63** 883-903, 1974.
5) Clementi F, Palade GE : Intestinal capillaries. I. Permeability to peroxidase and ferritin. J Cell Biol **41** : 33-58, 1969.
6) Friederici HHR, Taylor R, et al : The fine structure of capillaries in experimental scurvy. Lab Invest **15** : 1442-1458, 1966.
7) Graham RC, Karnovsky MJ Glomerular permeability. Ultrastructural cytochemical studies using peroxidase as protein tracers. J Exp Med **124** 1123-1134, 1966.
8) Graham RC Jr, Limpert S, et al : The uptake and transport of exogenous proteins in mouse liver. Ultrastructural cytochemical studies with peroxidase tracers. Lab Invest **20** 298-304, 1969.
9) Green WT Jr, Ferguson RJ: Histochemical and electron microscopic comparison of tissue produced by rabbit articular chondrocytes in vivo and in vitro. Arthritis Rheum **18** : 273-280, 1975.
10) Highton TC, Myers DB, et al: The intercellular spaces of synovial tissue. N Z Med J **67** : 315-325, 1968.
11) Karnovsky MJ The ultrastructual basis of capillary permeability studied with peroxidase as a tracer. J Cell Biol **35** 213-236, 1967.
12) Kushner I, Somerville JA : Permeability of human synovial membrane to plasma proteins. Relationship to molecular size and inflammation. Arthritis Rheum **14** : 560-570, 1971.
13) Mayerson HS, Wolfram CG, et al : Regional differences in capillary permeability. Am J Physiol **198** : 155-160, 1960.
14) Nettelbladt E, Sundblad L: On the significance of hyaluronic acid changes in the pathogenesis of joint effusion. Opuse Med **12** : 224-232, 1967.
15) Ogston AG, Phelps CF : The partition of solutes between buffer solutions and solutions containing hyaluronic acid. Biochem J **78** : 827-833, 1960.
16) Pappenheimer JR . Passage of molecules through capillary walls. Physiological Review **33** : 387-423, 1953.
17) Raviola E, Karnovsky MJ : Evidence for a blood-thymus barrier using electron-opaque tracers. J Exp Med **136** : 466-498, 1972.
18) Renke HG, Cotran RS, et al : Role of molecular charge in gromerular permeability. Tracer studies with cationized ferritins. J Cell Biol **67** : 638-646, 1975.
19) Sandson J, Hamerman D : Paper electrophoresis of human synovial fluid. Proc Soc Exp Biol Med **98** 564-566 1958.
20) Schneeberger EE, Karnovsky MJ : The influence of intravascular fluid volume on the permeability

of newborn and adult mouse to ultrastructural protein tracers. J Cell Biol **49** : 319-334, 1971.
21) Schumacher HR Jr: The microvasculature of the synovial membrane of the monkey : Ultrastructural studies. Arthritis Rheum **12** 387-404, 1966.
22) Schur PH, Sandson J : Immunologic studies of the proteins of human synovial fluid. Arthritis Rheum **6** . 115-129, 1963.
23) Shannon L, Graham RC Jr : Protein uptake by synovial cells. I. Ultrastructural study of the fate of intraarticularly injected peroxidase. J Histochem Cytochem **19** . 29-42, 1971.
24) Simionescu N, Siminonescu M, et al Permeability of intestinal capillaries. Pathway followed by dextrans and glycogens. J Cell Biol **53** : 365-392, 1972.
25) Simionescu N, Simionescu M, et al : Permeability of muscle capillaries to exogenous myoglobin. J Cell Biol **57** : 424-452, 1973.
26) Simionescu M, Simionescu N, et al : Morphometric data on the endothelium of blood capillaries. J Cell Biol **60** : 128-152, 1974.
27) Simkin PA, Pizzorno JE : Transsynovial exchange of small molecules in normal human subjects. J Appl Physiol **36** : 581-587, 1974.
28) Southwick WO, Bensch KG : Phagocytosis of colloidal gold by cells of synovial membrane. J Bone Joint Surgery **53**-A 729-741, 1971.
29) Suter ER, Majno G Ultrastructure of the joint capsule in the rat Presence of two kinds of capillaries. Nature **202** : 920, 1964.
30) Vegge T : An electron microscopic study of the permeability of iris capillaries to horseradish peroxidase in the Velvet monkey. Z Zellforsch **121** : 74-81, 1971.
31) Venkatachalam MA, Fahimi HD : The use of beef liver catalase as a protein tracer for electron microscopy. J Cell Biol **42** : 480-489, 1969.
32) Venkatachalam MA, Karnovsky MJ, Extravascular protein in the kidney. An ultrastructural study of its relation to renal peritubular capillary permeability using protein tracers. Lab Invest **27**: 435-444, 1972.

Portions of this work were presented at the Annual Meeting of the American Rheumatism Association, Chicago, Illinois, June 9-11, 1976. Abstract in Arthritis and Rheumatism **19** : 800, 1976.
Chiaki Hamanishi, M.D. : Postdoctoral course of Orthopaedic Surgery and Pathology, Faculty of Medicine, Kyoto University.

和文抄録

血液一関節関門の電子顕微鏡学的研究

——5種類の電顕的トレーサーを用いて——

京都大学整形外科学教室（主任：山室隆夫教授）
浜　西　千　秋

正常関節液中に含まれる蛋白分子は，アルブミン等の低分子の蛋白が多く含まれ IgM 等の大分子蛋白は血漿中のわずか数%しか含まれていない．又フィブリノーゲンのような非対称形分子は含まれない．このように，血漿蛋白の透過を選択的に制限する機構が関節滑膜に存在すると考えられ，これを血液—滑膜関門（Blood-Synovial Barrier, B. S. B）と名付けた．そして関節滑膜のどのような形態学的特徴が B. S. B に相当するのかを明らかにする為に，マウス膝関節滑膜における微細構造を電顕的に観察し，同時に，尾静脈より，分子量，分子サイズの異る5種類の電顕的トレーサーを注入し，滑膜血管腔より，関節腔に到る透過動態を経時的に観察した．トレーサーとして peroxidase, catalase, ferritin, glycogen, dextran 200, を用いた．これらによって以下の点が明らかとなった．

1．関節滑膜には areolar, adipose, fibrous, muscular の4タイプが認められた．2．滑膜表層細胞層には旺盛な貪食能を有する“A”細胞，線維芽細胞類

似の "B" 細胞，そして "B" 細胞が活発化して特徴的な形態を示したと考えられる "C" 細胞等が観察された．3．滑膜最表層の毛細血管に，関節腔に面して有窓内皮をしばしば認めたが，ここからのトレーサーの流出は認められなかった．4．滑膜基質を，ルテニウムレッドで染色する事により，ヒアルロン酸—蛋白複合体（proteoglycan）とコラーゲンとの密接な関係が明らかとなった．5．B. S. B として次の3段階が明らかとなった．1）滑膜小血管内皮細胞，及び細胞間隙の，分子サイズ，分子形態，電荷に対する，機能的，構造的選択透過能力．これは peroxidase, ferritin 等と catalase という非対称形分子との著明な透過動態の差違により明らかとなった．

2）血管外基底膜の，分子サイズ200Å以上，Effective difusion radius 100Å 以上の分子に対するバリヤー効果．これはデキストラン分子の透過動態より明らかとなった．3）血管周囲のマクロファージ，及び滑膜表層 "A" 細胞による，極めて旺盛な蛋白取り込み能力．これらは peroxidase, ferritin, dextran 等で観察された．6．基質に存在する，ヒアルロン酸—蛋白複合体による "excluded volume effect" は今日まで主要な B.S B と考えられてきているが，血管外に移送された peroxidase や ferritin の滑膜基質における分布は均一であり，このような "effect" は観察されなかった．